Eur. Phys. J. B **22**, 11–16 (2001)

THE EUROPEAN PHYSICAL JOURNAL B

EDP Sciences

Melting of the cooperative Jahn-Teller distortion in $LaMnO_3$ single crystal studied by Raman spectroscopy

L. Martín-Carrón[a] and A. de Andrés

Instituto de Ciencia de Materiales de Madrid (Consejo Superior de Investigaciones Científicas) Cantoblanco, 28049 Madrid, Spain

Received 25 January 2001 and Received in final form 14 March 2001

Abstract. We have studied the behavior of the Raman phonons of a stoichiometric $LaMnO_3$ single crystal as a function of temperature in the range between 77 K and 900 K. We focus on the three main phonon peaks of the Pbnm structure, related to the tilt, antisymmetric stretching (Jahn-Teller mode) and stretching modes of Mn-O octahedra. The phonon frequencies show a strong softening that can be fit taking into account their renormalization because of three phonon anharmonic effects in the pseudoharmonic approximation. Thermal expansion effects, in particular the variation of Mn-O bond lengths with temperature, are not relevant above 300 K. On the contrary, phonon width behavior deviates from the three phonon scattering processes well bellow T_c. The correlation between the magnitude of the cooperative Jahn-Teller distortion, that disappears at 800 K, and the amplitude of the Raman phonons in the orthorhombic phase is shown. Nevertheless, Pbnm phonons are still observable above this temperature. Phonon width and intensity behavior around T_c can be explained by local melting of the orbital order that begins quite below T_c and by fluctuations of the regular Mn-O octahedra that correspond to dynamic Jahn-Teller distortions.

PACS. 63.20.-e Phonons in crystal lattices – 75.30.Vn Colossal magnetoresistance

1 Introduction

Doped manganese perovskites $R_{1-x}A_xMnO_3$ (R = La, Nd or Pr, A = Ca, Sr, Ba...) have recently attracted much interest because of the high values of the magnetoresistance that many of these compounds present [1]. The strong change in the conductivity by an external magnetic field is due to the close relation between magnetic order and electronic conduction in doped materials with divalent cations or non-stoichiometric samples. Many of these compounds order ferromagnetically at some temperature below about 330 K and become metallic. Some of them present a charge order transition accompanied by an insulating behavior and antiferromagnetic order. Phase segregation, stripes and many subtle spin or/and orbital orders are present in these compounds revealing the delicate equilibrium between different competing interactions. The metallic-ferromagnetic state has been explained by the double exchange interaction mechanism that enhances the conductivity by aligning the localized spins of two neighboring Mn ions through the spin of the hopping e_g electron. But electron-phonon and Jahn-Teller interactions have to be considered to explain many of the previously described behaviors. Stoichiometric $RMnO_3$ compounds with the Pbnm orthorhombic structure present a strong Jahn Teller cooperative distortion of the Mn-O octahedra related to the orbital ordering of Mn e_g levels. The $LaMnO_3$ compound is antiferromagnetic below 135 K and undergoes at 800 K a structural transition to the nearly cubic perovskite that has been described as rhombohedral, monoclinic or orthorhombic. A detailed study of a stoichiometric sample [2] shows that above 800 K the cooperative Jahn-Teller order disappears but dynamic Jahn-Teller fluctuations are still present. The importance of the phonons is often invoked and proved by the drastic observed isotope effects [3], but the Raman spectra of doped compounds are still not deeply understood. Raman phonons have been studied in orthorhombic $LaMnO_3$ single crystals [4,5], and, in Sr doped [5–7] and Ba doped compounds [8], as well as in Ca doped pellets [6,9] and thin films [10]. Several of these works report the effect of the oxygen content and the rhombohedral structure on the Raman features. The low temperature Raman spectra of a pure compound show a softening of the stretching mode below the magnetic transition [11]. Recently Dediu *et al.* [12] report the appearance of two peaks, below the charge order temperature in $Pr_{0.65}Ca_{0.35}MnO_3$, related to the unit cell doubling along a-axis, and assign the change in the slope of the dependence of the peak frequency and width *vs.* temperature to the transition from dynamical to static Jahn-Teller (JT) distortions. The relation between the shape of the Raman phonons and the JT distortion is often appealed to but not explained. The principal problem is that Raman phonons are sensitive to locally

[a] e-mail: lauram@icmm.csic.es

distorted octahedra as well as to dynamical disorder. Both kinds of deviations from the random structure are difficult to be evaluated with diffraction techniques. Pair density function analysis of pulsed Neutron diffraction data show that local JT distortions occur in Sr doped $LaMnO_3$ in both paramagnetic and metallic phases [13]. X-ray diffuse scattering, observed in the paramagnetic regime of a doped manganite [14], has been related to local lattice distortions (Jahn-Teller distortions) due to the localization of electrons on Mn sites.

With the conviction that static and dynamical Jahn-Teller distortions related to Mn^{3+} ions are crucial in the understanding of Raman phonons and of the properties of doped or non-stoichiometric compounds, we have carefully studied the Jahn-Teller transition of a stoichiometric $LaMnO_3$ single-crystal where diffraction studies have described in detail the structural changes through this transition (and where the low temperature Raman spectra are well understood). In the present work the correlation between the structural changes and the phonons are clearly evidenced. The composition of the sample is of basic importance because the presence of a small amount of Mn^{4+} ions disturbs the system so much that the structure and the magnetic order can be different from those corresponding to the stoichiometric compound. Phonons, and in particular their widths, present important changes even for compounds with light Mn^{4+} doping.

2 Experimental details

The single crystal studied here has been prepared by the floating zone method [2]. It exhibits the Pbnm orthorhombic structure ($D2h^{16}$, with $Z = 4$) and orders antiferromagnetically at 135 K as it corresponds to a sample with the correct stoichiometry [2]. Raman spectra were obtained with a Renishaw Ramascope with CCD detector and excited with the 514.5 nm line of an Ar^+ laser. The spectra were recorded at temperatures between 900 K and 77 K in the backscattering geometry with an Olympus microscope. Below 300 K we used a continuous flow Oxford Instrument cryostat and above 300 K the spectra were obtained from the sample located inside a Linkem TS-1500 furnace. All spectra have been corrected by the spectral response of the experimental set-up.

The single crystal possesses domains with the c-axis oriented along any of the three axes of the underlying cubic perovskite [15]. The spectra have been obtained with a $\times 10$ objective (focus diameter larger than 10 micron) and low laser power (about 1 mW) in order to avoid heating the sample locally by the laser beam. Increasing the power of the beam to 4 mW leads to a local overheating estimated to be about 100 K.

3 Results and discussion

The Raman active modes of the Pbnm structure (mirror plane "m" is perpendicular to the long c-axis) are:

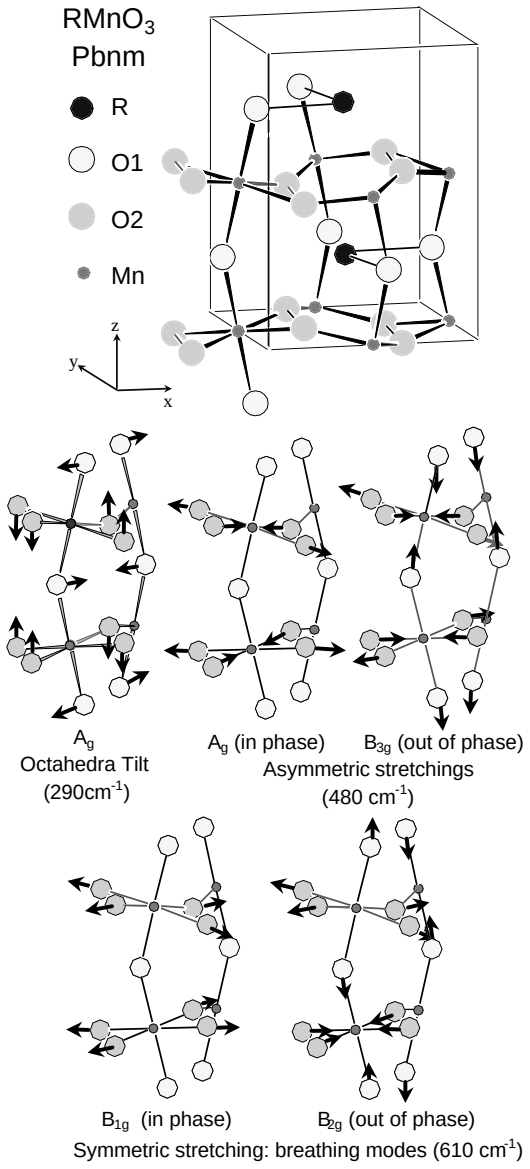

Fig. 1. Pbnm structure and several relevant Raman normal modes of $LaMnO_3$.

$7A_g+7B_{1g}+5B_{2g}+5B_{3g}$ and the non-zero components of the Raman tensors are: $(xx,\ yy,\ zz)$, (xy), (xz) and (yz) for A_g, B_{1g}, B_{2g} and B_{3g} representations respectively. But, when choosing the Pnma coordinate system, the normal modes are classified in the following way: $7A_g+5B_{1g}+7B_{2g}+5B_{3g}$ [4]. Now, the Raman tensor component of the B_{1g} modes is (xz) and that of the B_{2g} is (xy). This means that the B_{1g} modes in the Pbnm system corresponds to the B_{2g} representation in the Pnma setting. We consider it necessary to stress this point because some controversy and confusion has been detected in the literature. Here, we have chosen the Pbnm axes orientation (Fig. 1). In this case, La and O(1) (apical) ions do not move along the c-axis direction for $2A_g+ 2B_{1g}$ modes

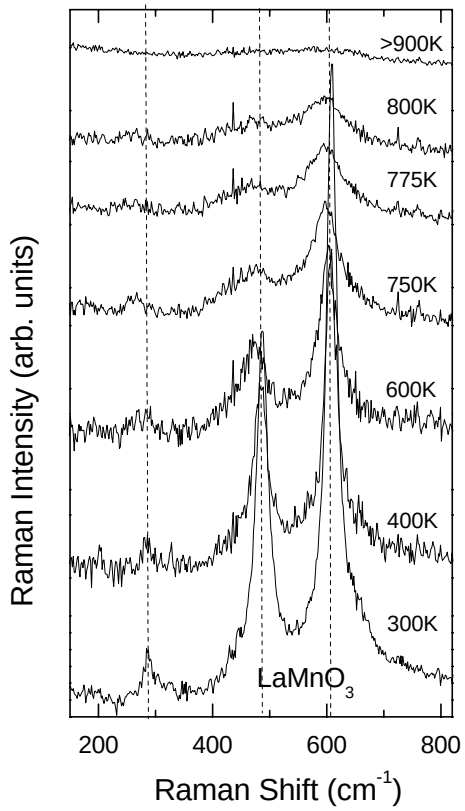

Fig. 2. Raman spectra from 300 K to 900 K of a stoichiometric $LaMnO_3$ single-crystal.

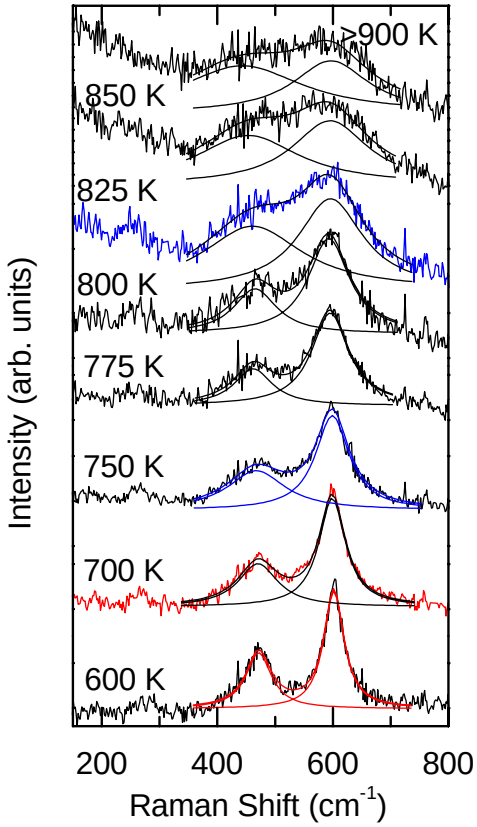

Fig. 3. Raman spectra of a $LaMnO_3$ single-crystal bellow and above the Jahn-Teller structural transition. Continuous lines are the fits to the phonons. The intensity scales of the spectra have been changed for a better visualization.

corresponding to each of them. In plane oxygen ions O(2) have no such limitation and Mn ions do not participate to Raman modes because located at inversion centres. Also, A_g normal modes of O(2) ions consist in "in phase" movements of the ions from $z = 0$ and $z = 0.5$ planes, while B_{3g} are the same movements but "out of phase". The same correspondence occurs for B_{1g} (in phase) and B_{2g} (out of phase) modes. Therefore, because these O(2) ions corresponds to different octahedra, their frequencies are expected to be very similar.

The main features of the $LaMnO_3$ Raman spectrum (Fig. 2) correspond to high frequency peaks around 480 cm^{-1} and 610 cm^{-1} that pertain to different Mn-O bond-stretching modes and to a region around 300 cm^{-1} which corresponds to different tilts of the Mn-O octahedra. In Figure 1 we present the symmetry and atomic displacements of the main peaks. The symmetry of 480 and 610 cm^{-1} peaks have been determined to be (in the Pbnm setting) A_g and B_{1g} respectively [4]. The atomic movements in Figure 1 are somewhat different from those proposed by Iliev *et al.* [4]. In particular we propose a Jahn-Teller type mode for the 480 cm^{-1} peak as we will discuss further.

Figure 2 shows the evolution of the Raman phonons from 300 K to 900 K, well above the structural transition. An important shift to lower values of the phonon frequencies is observed together with a dramatic increase of the widths and decrease of peak intensity. Figure 3 presents the fits to the spectra in the temperature range between 600 and 900 K.

The simplest approximations to anharmonic effects are the quasiharmonic and pseudoharmonic ones [16,17]. The first one takes into account the changes in the phonon frequencies with temperature due to the modification of the interatomic forces because of thermal expansion. The simplest approach to anharmonic decay of optical phonons is the pseudoharmonic approximation where, in fact, each phonon is considered as independent but with a renormalized energy and a finite lifetime due to anharmonic interactions [18]. The validity of this model is limited to high energy phonons and long lifetimes, *i.e.* when the phonon-phonon interaction is small compared to their energies.

In order to estimate the importance of both terms in the observed dependence with temperature of the phonon frequencies and widths (related to phonon lifetimes) we have evaluated the expected changes in the phonon frequencies caused by the variation of the interatomic distances in the crystal. Figure 4a shows the observed changes with temperature of the frequencies of the three previously described modes normalized to their values at 300 K. We have also included the measured frequencies below RT from [11] (open symbols in the figure).

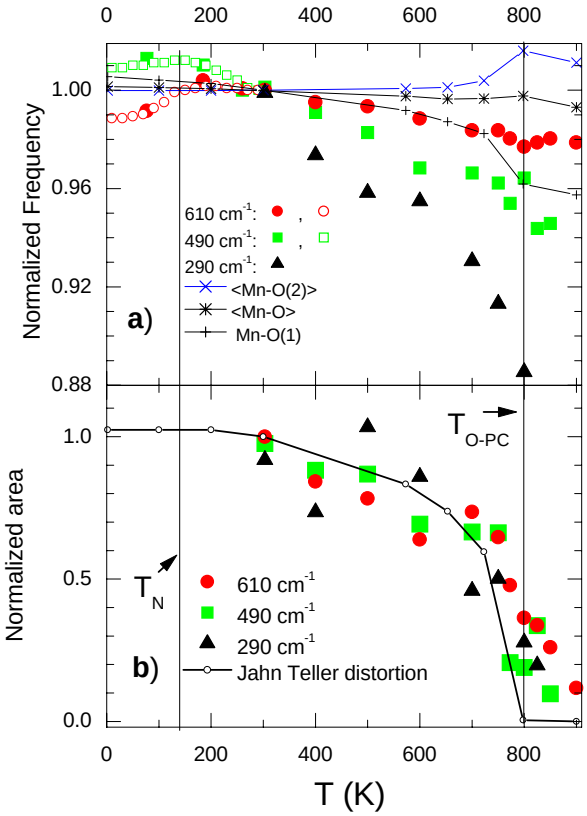

Fig. 4. (a) Frequencies of the tree main Raman peaks, as function of temperature, normalized to their 300 K values, and the expected behavior from quasiharmonic (thermal expansion) effects as explained in the text. (b) Normalized intensities of the three peaks and Jahn Teller distortion (continuous line) obtained from structural data of reference [2].

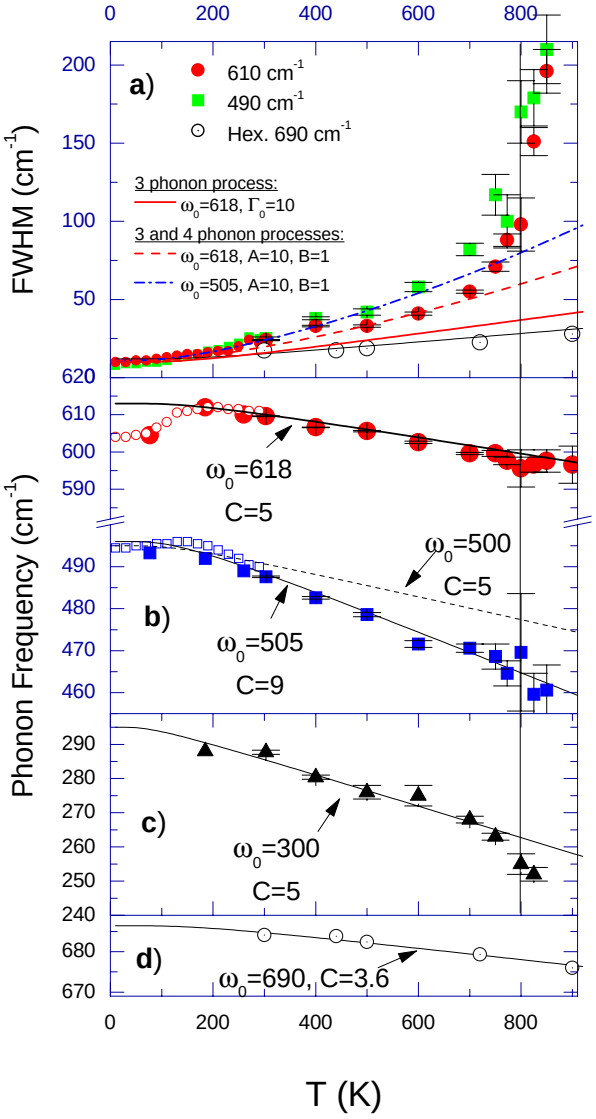

Fig. 5. Main Raman phonon widths (a) and frequencies (b) and (c) as a function of temperature of stoichiometric $LaMnO_3$. (a) and (d) present data for hexagonal $YMnO_3$. The lines are width and frequency behaviors expected from three or four phonon scattering processes. The fit parameters are given in each case.

The anomalous softening below T_c, for the 610 cm^{-1} peak, was interpreted in terms of a spin-phonon coupling caused by a modulation of the superexchange integral.

Taking into account a simple model for the force constants: $K = F_{ij}/r_{ij}^3$, and $\varpi = \sqrt{(K/m)}$, where F_{ij} are constants that depend on i and j ions, and r_{ij} are, in the present case, Mn-O distances, we can estimate the changes in the stretching modes (at 610 and 480 cm^{-1}) due to the changes with temperature of these distances obtained from [2]. The continuous lines of Figure 4a represent the quasiharmonic effects due to the changes in the mean value of in-plane Mn-O(2) distances, to the changes in the mean value of the three Mn-O distances and that due to the apical oxygen bond Mn-O(1). The symmetries of the observed 490 and 610 cm^{-1} modes (A_g and B_{1g}, respectively) do not allow O(1) motion along c-axis, therefore the Mn-O(1) bonds are not involved in these movements.

The figure shows that structural changes occurring as the temperature increases tend to increase the stretching modes frequencies contrary to the observed strong decrease. It is clear that the dominant mechanism for frequency shift is anharmonic scattering of phonons, which is also the expected mechanism for peak broadening. In particular, the most probable mechanism is the three phonon one where one phonon relaxes into two phonons of the same energy [17]. A simplified approximation to its very complicated formulation [18] leads to the following formula for the damping constant (related to peak width and inversely proportional to phonon lifetime) and phonon frequency shift [19]: $\Gamma(T) = \Gamma_0(1 + \frac{2}{e^x-1})$ and $\varpi(T) = \varpi_0 + C(1 + \frac{2}{e^x-1})$ where $x = \hbar\varpi/2k_BT$. Fits to experimental frequencies and widths of the renormalized values considering three phonon scattering processes are presented in Figure 5. It can be observed that the fit of the frequencies with two parameters (one of which is the 0 K frequency) is very good except very near the JT structural transition. Notice also that "C" parameter, which is related to the strength of phonon coupling, is, for the here

called JT phonon, about twice that corresponding to both other phonons.

On the other hand, the three phonon expression for the lifetime cannot fit the observed behavior of the peak width. We have included, for comparison purposes, the experimental and fitted data, Figures 5a and 5d, of $YMnO_3$ in its hexagonal phase and we can observe that both frequency and width follow perfectly the expected behavior. The upper part of Figure 5 includes also, represented as dashed lines, the combination of three and four phonon scattering processes showing a better agreement with experimental data but that, in fact, is only due to a larger number of fitting parameters. In any case, the fits become bad above 700 K specially for the JT mode.

In Figure 4b we present the integrated intensity of the three modes corrected by the thermal factor $(1+n(\varpi, T))$ corresponding to first order Raman Stokes phonons. We would then expect a temperature independent intensity but observe a strong decrease. In the present case there is a structural phase transition at about 800 K to a quasi-cubic structure and, taking into account that a cubic perovskite has no Raman modes allowed, the Raman peaks are expected to disappear at or near the phase transition temperature. The observed intensities of the three modes start to decrease slightly above 300 K. The continuous line of Figure 4b represents the behavior of (a-b) (lattice parameters) which is related to the static Jahn Teller distortion due to orbital ordering. The direct measure of the static Jahn-Teller distortion is the comparison between Mn-O(2) distances whose difference behaves in the same manner (see data of Ref. [2]) as (a-b). The correlation between the Jahn-Teller distortion and the phonon intensity is very good over a large temperature range. Nevertheless, at and above the phase transition temperature, when Mn-O octahedra are regular according to diffraction data, the peaks are still observable (Fig. 3). At this moment the cooperative static charge order has disappeared but fluctuations of Mn-O octahedra, that is dynamic Jahn-Teller distortions, are occurring. Because the Raman process is very rapid it is possible to see an instantaneous picture of the lattice where the octahedra present many slightly different bond lengths and angles. These fluctuations lower the Mn-O octahedra symmetry allowing observation of the Raman modes.

In the orthorhombic phase, the departure of the behavior of the phonon width from that expected for the previously discussed phonon scattering processes can be understood considering that dynamic fluctuations of octahedra, and therefore, local melting of the orbital order, are happening at temperatures well below the structural phase transition. These dynamical Jahn-Teller distortions broaden Raman peaks in a similar way of an inhomogeneous broadening due to a distribution of octahedron configurations. These processes will contribute to the width of the phonon peaks but do not affect the peak frequency whose values correspond to the average structure.

4 Conclusions

The main Raman phonons of a stoichiometric $LaMnO_3$ single crystal have been related to Mn-O octahedra movements. All peaks show a strong shift to lower energies above 300 K that can be explained by three phonon scattering processes that renormalize their frequencies. The parameter related to phonon-phonon coupling is nearly twice for the here-called Jahn-Teller phonon than for the other modes, tilt and symmetric in plane Mn-O(2) stretching. The effect of the lattice expansion on the phonon frequencies has been estimated taking into account the variation of bond lengths and is found to be very small. The widths of all peaks present a very strong increase that do not follow the three phonon scattering model. The fit is better considering three and four phonon scattering processes but fails above 700 K, in particular for the Jahn-Teller mode. The integrated intensity of all peaks decreases drastically above 300 K following very well the evolution of the magnitude of the static Jahn-Teller distortion except above the structural transition where a remaining spectral weight is observed up to, at least, 900 K, indicating that dynamic Jahn-Teller distortions are occurring. Our observations indicate that melting of the orbital order is beginning well below the transition temperature; probably as local fluctuations of Mn-O octahedra. The distribution of bond lengths and angles of the octahedra increases with temperature, as noted by the increasing width of the Raman peaks. Therefore we have quantitatively demonstrated the correlation between the magnitude of the static Jahn-Teller distortion and the amplitude of the Raman phonons in the orthorhombic phase. The deviation of the phonon-widths from anharmonic decay and of the intensity from JT static distortion, around the structural transition temperature, are related to the local melting of the orbital order in the orthorhombic phase and to fluctuations of the regular Mn-O octahedra (dynamic Jahn-Teller distortions) in the pseudo-cubic phase.

We thank J. Rodríguez-Carvajal for supplying the sample. This work was supported by CICyT under contract MAT2000-1384 and by Comunidad Autonoma de Madrid under contract 07N/0027/1999. L. M-C thanks CSIC and Lasing S.A. for financial support.

References

1. S. Jin, T.H. Tiefel, M. McCormack, R.A. Fastnacht, R. Ramesh, L.H. Chen, Science **264**, 413 (1994).
2. J. Rodríguez-Carvajal, M. Hennion, F. Moussa, A.H. Moudden, L. Pinsard, A. Revcolevschi, Phys. Rev. B **57**, R3189 (1998).
3. N.A. Babushkina, L.M. Belova, O.Y. Gorbenko, A.R. Kaul, A.A. Bosak, V.I. Ozhogin, K.I. Kugel, Nature **391**, 159 (1998).

4. M.N. Iliev, M.V. Abrashev, H.G. Lee, V.N. Popov, Y.Y. Sun, C. Thomsen, R.L. Meng, C.W. Chu, Phys. Rev. B **57**, 2872 (1998).
5. V.B. Podobedov, A. Weber, D.B. Romero, J.P. Rice, H.D. Drew, Phys. Rev. B **58**, 43 (1998).
6. E. Granado, N.O. Moreno, A. García, J.A. Sanjurjo, C. Rettori, I. Torriani, S.B. Oseroff, J.J. Neumeier, K.J. McClellan, S.W. Cheong, Y. Tokura, Phys. Rev. B **58**, 11435 (1998).
7. P. Bjornsson, M. Rubhausen, M. Kall, S. Eriksson, J. Eriksen, L. Borjesson, Phys. Rev. B **61**, 1193 (2000).
8. C. Roy, R.C. Budhani, J. Appl. Phys. **85**, 3124 (1999).
9. A. de Andrés, J.L. Martínez, J.M. Alonso, E. Herrero, C. Prieto, J.A. Alonso, F. Agulló, M. García-Hernández, J. Mag. Mag. Matter. **196-197**, 453 (1999).
10. V.B. Podobedov, D.B. Romero, A. Weber, J.P. Rice, R. Schreekala, M. Rajeswari, R. Ramesh, T. Venkatesan, H.D. Drew, Appl. Phys. Lett. **73**, 3217 (1998).
11. E. Granado, A. García, J.A. Sanjurjo, C. Rettori, I. Torriani, F. Prado, R.D. Sanchez, A. Caneiro, S.B. Oseroff, Phys. Rev. B **60**, 11879 (1999).
12. V. Dediu, C. Ferdeghini, F.C. Matacotta, P. Nozar, G. Ruani, Phys. Rev. Lett. **84**, 4489 (2000).
13. D. Louca, T. Egami, E.L. Brosha, H. Roder, R. Bishop, Phys. Rev. B **56**, R8475 (1997).
14. S. Shimomura, N. Wakabayashi, H. Kuwahara, Y. Tokura, Phys. Rev. Lett. **83**, 4389 (1999).
15. J. Rodríguez-Carvajal (private communication).
16. *The Physics of Phonons*, edited by J.A. Reissland (John Wiley and Sons Ltd., Bristol, 1973), Chaps. 4 and 6.
17. *The Physics of Phonons*, edited by G.P. Srivastava (Adam Hilger-IOP publishing Ltd., Bristol, 1990), Chap. 6.
18. P.G. Klemens, Phys. Rev. **148**, 845 (1966).
19. M. Balkanski, R.F. Wallis, E. Haro, Phys. Rev. B **28**, 1928 (1983).